

## Strain geometry, microstructure and mineral chemistry in metagabbro shear zones: a study of softening mechanisms during progressive mylonitization

M. J. WATTS

p/a Nam Assen, Schepersmaat 2, 9405 TA Assen, The Netherlands

and

G. D. WILLIAMS

Department of Geology, University College,  
P.O. Box 78, Cardiff CF1 1XL, U.K.

(Received 14 April 1982; accepted in revised form 2 February 1983)

**Abstract**—The strain geometry, microstructure and metamorphism is described from two minor shear zones from the Chatelaudren metagabbro, N. Brittany. A serially slabbed shear zone reveals a strain geometry consistent with simple shear deformation. Strain calculations based on  $X$  trajectory angles coincide with those obtained from elliptical mineral clusters at high values of strain only. Strain profiles typically show a broad low-strain region with a narrow high-strain peak at the centre of the zones. Microstructures typically show distinct grain size reduction in both amphibole and feldspar towards the high strain region of shear zones, and this is discussed in terms of deformation mechanisms related to strain softening. A palaeostress estimate based on recrystallized feldspar grain sizes gives a differential stress of 32 MPa for the low strain region and 119 MPa in the shear zone centre. Electron probe analyses reveal chemical and mineralogical changes accompanying metamorphism within the shear zones. This suggests local conditions favourable for ionic diffusion and the activity of fluids is implied.

### INTRODUCTION

SHEAR ZONES are simply displacement zones within which rocks deform as a volume constant continuum. They are characterized by large strains when compared to the surrounding 'average strain' or the more easily definable undeformed state. A recent definition for a shear zone, which is followed here, is that proposed by White *et al.* (1980) which states that a shear zone is "a planar zone of concentrated, dominantly simple shear deformation which helps to accommodate or wholly accommodates an imposed regional or local strain rate which the country rock cannot accommodate by bulk deformation".

Although variations in intensity of deformation from locality to locality within deformed regions have been appreciated for a long time (e.g. Teall 1885, Peach *et al.* 1907), it was the influential paper of Ramsay & Graham (1970) that instigated a spate of studies on shear zones through the 1970s.

Such studies fall into three main categories: (1) the strain geometry of shear zones (e.g. Ramsay & Graham 1970, Coward 1976), (2) the development of mylonites in shear zones (e.g. White 1976, Carreras *et al.* 1977) and (3) chemical and mineralogical changes accompanying metamorphism in shear zones (e.g. Beach & Fyfe 1972, Beach 1976, 1980).

In this paper, we describe in some detail the strain geometry, the progressive mylonitization in terms of

microstructure and the metamorphic changes in two minor shear zones from a metagabbro body, the Chatelaudren Metagabbro, from N. Brittany (Fig. 1). We attempt to show the interrelationships between strain geometry and microstructure and discuss them in terms of strain softening mechanisms. The role of fluids in metamorphism is considered.

The two shear zone samples were collected from a recent road cut through metagabbro on the St. Briec road (RN12) which meant that the rocks were sufficiently fresh for meaningful geochemical analysis. Shear zone 1 was large enough (8 cm × 42 cm) to be serially slabbed parallel to the  $XZ$  plane of the zone (Fig. 2a) which allowed geometrical strain analysis. Two thin sections were also made for electron probe analysis, one from a high-strain region, and one from a low-strain region of slab 1. Shear zone 2 was small (2 cm across), and could be mounted on a single thin section cut parallel to the  $XZ$  plane. Using this, detailed microstructural observations, and probe analyses were made.

### THE CHATELAUDREN METAGABBRO

The Chatelaudren metagabbro (Fig. 1) is a basic intrusion presently considered to represent Pentevrian basement within the Cadomian block of the Armorican massif (Leutwein *et al.* 1968, Cogné 1976, Roach 1977). It has been variously interpreted as a suite of syenites

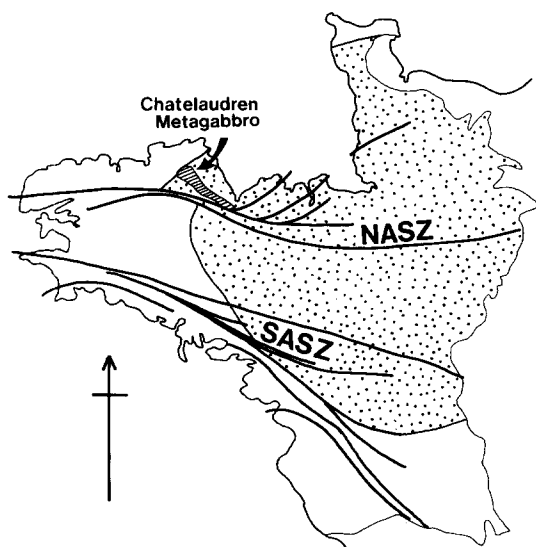


Fig. 1. Location map for the Chatelaudren metagabbro in the Armorican massif. NASZ, North Armorican Shear Zone System; SASZ, South Armorican Shear Zone System. Cadomian (~ 600 Ma) basement stippled.

(Barrois 1896), dioritic gneisses and gneissic diorites (Cogné 1976). However, these rocks are best described as amphibolitized metagabbros. This metagabbro is structurally simple, containing a weakly developed main foliation which varies in intensity throughout the outcrop and is weakest near Chatelaudren where primary igneous features are preserved.

Chemically, the rocks are basic, being olivine + hypersthene or quartz + hypersthene normative. Macroscopically, the gabbro is a coarse grained, holocrystalline rock with hypidiomorphic texture made up of mafic and felsic aggregates 3–6 mm in diameter. Essentially, it is a two phase assemblage of calcic plagioclase (45–50%) and green hornblende (40–50%) forming the polycrystalline aggregates whose alignment defines the weak main foliation. The most important accessories with their typical modal ranges are biotite (2–5%), ilmenite (1–4%), quartz (2–4%) and sphene (1–5%). Pyroxenes, which occur in chemical norms are never preserved and have been completely pseudomorphed by poikiloblastic hornblende + quartz; a very common feature of metagabbro (e.g. Thayer 1980, p. 276). Following the initial amphibolitization, the gabbro variously shows signs of modification by metamorphism. Large single hornblendes are partially or completely replaced by a mosaic of smaller hornblendes, biotite alters to chlorite, feldspars develop undulose extinction and suffer patchy sericitization, and twinning on the pericline law becomes important. Following the criteria of Miyashiro (1978, p. 249–254), the metamorphic mineral assemblages prove amphibolite facies metamorphism in that the hornblende remains stable throughout, and the calcic content of the plagioclase does not fall below  $An_{30}$ . The presence of chlorite and clinozoisite/epidote in some varieties indicates that the metamorphism shows variable effects of retrogression.

## STRAIN GEOMETRY

A sample of a shear zone (Shear Zone 1) was serially slabbed parallel to the  $XZ$  plane (Fig. 2a) to enable a comparison of strain measurements at different intervals along the intermediate  $Y$  axis and to test for departures from simple shear. For preliminary investigation simple shear is assumed.

The most important structure to locate is the shear zone boundary plane (which is, or is parallel to, the shear plane), for all angular measurements are made relative to it and location errors of a few degrees can result in large fluctuations of estimated shear strain ( $\gamma$ ) values. Although in the literature, difficulties in assessing the precise position of boundary planes have not been specified, problems do arise in view of the likelihood of the first mesoscopically visible deformation effects lying inside the 'real' shear zone boundary (Hara *et al.* 1973, Burg & Laurent 1978). The shear zone border was determined by a line joining aggregates immediately outside of those that show the first indications of an orientated shape fabric.

Shear zone 1 presents a further complexity in that the shear zone itself is slightly curvilinear about an axis parallel to  $Y$ . The main deflection in direction shown by the shear zone (most marked in the high strain regions) is about 7° and occurs approximately midway along its length. It is obvious that this deviation must be taken into account if parity of shear strain values across the zone is to be maintained. The most feasible solution was to select two boundary surfaces with a constant angular separation of 7°.

Felsic and mafic mineral aggregates are somewhat irregular in shape (especially at low strains) but it has been usual to treat similar aggregates as approximate ellipsoids and assume that they were spheres in the undeformed state (Coward 1976, Burg & Laurent 1978).

A general tracing of the foliation based on orientations of mineral aggregates was completed for all four slabs. On average, 200 locations on these  $X$  trajectories from each slab were used to estimate shear strain values ( $\gamma$ ) as follows: The angle between the  $X$  trajectory and the shear zone boundaries ( $\theta$ ) was measured at each location. Shear strain is given by:

$$\gamma = \frac{2}{\tan 2\theta} \quad (\text{after Ramsay \& Graham, 1970}). \quad (1)$$

A grid sample of  $\gamma$  values for each slab could then be contoured, but, because of high strains, the contour pattern was indistinct in the shear zone centre. This was resolved by contouring  $\ln \gamma$  values (Fig. 2b). Such natural log contours enable more precise shear strain definition towards the high-strain zone centre.

Various traverses across the four slabs (Fig. 2b) were used to construct distance versus strain profiles (Fig. 3). The four profiles taken along the length of slab 3, as well as those from the other sections, all record a similar shape, characterized by a broad region of low strain with a very narrow central region of high strain.

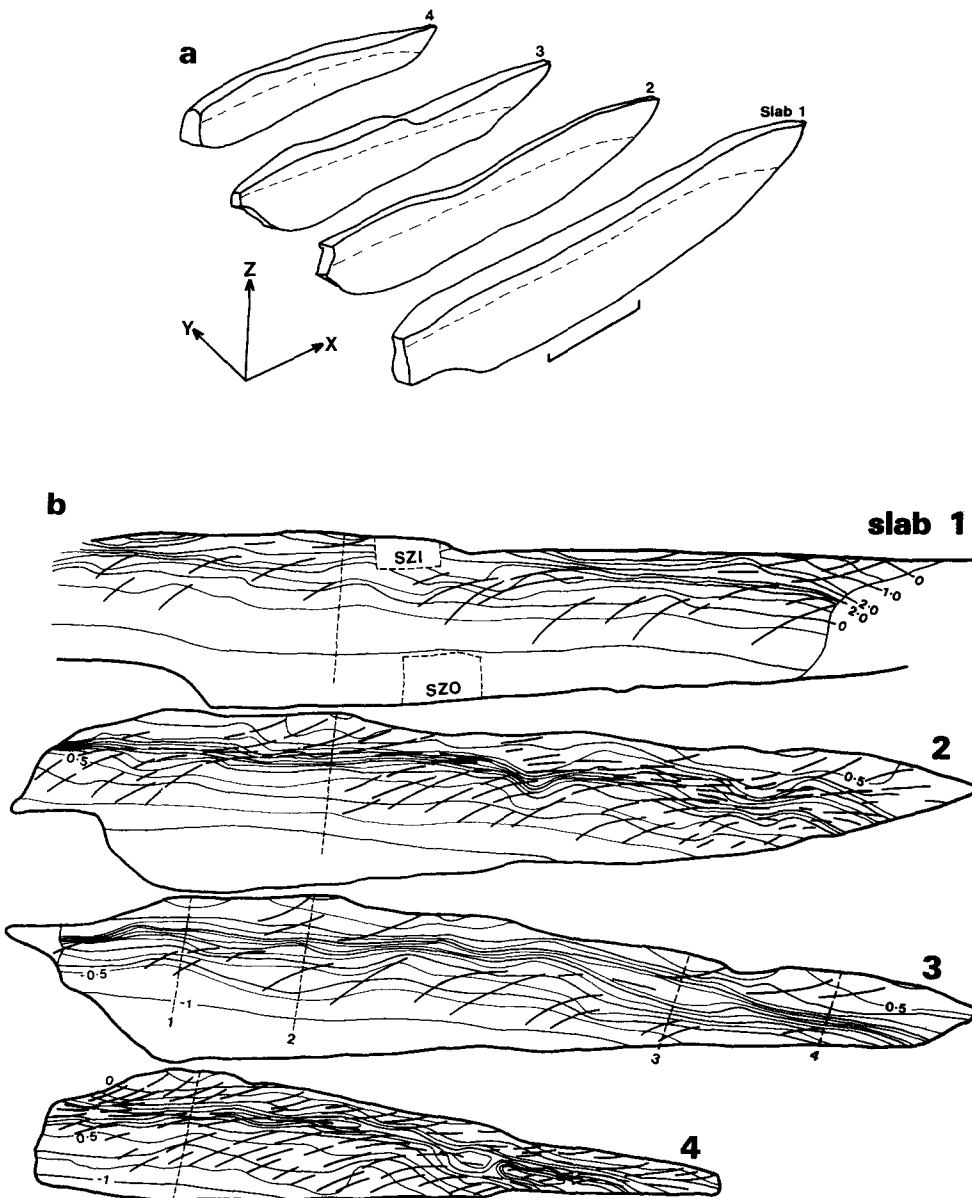


Fig. 2. (a) Isometric sketch of serially slabbed shear zone 1 and relationship of slabs with principal shear zone axes. Dashed lines indicate shear zone centre. Scale bar 10 cm. (b) Foliation trajectories and contours of natural log  $\gamma$  values of four slabs. Dashed lines indicate location of strain profiles of Fig. 3; SZ0 and SZ1 are locations of the probed thin sections.

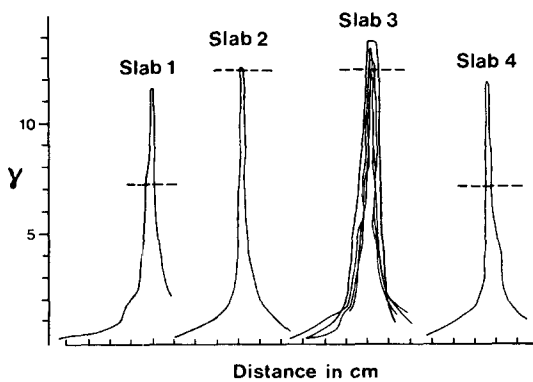


Fig. 3. Distance vs shear strain profiles across the four slabs. The dashed line across each profile signifies the highest equivalent  $\gamma$  value obtained from the marked  $\ln \gamma$  contours.

The  $X/Z$  strain ratio ( $R$ ) can be measured for individual mineral aggregates and plotted against  $\theta$  (Fig. 4a). Beyond ratios of 15 or 20:1,  $R$  is difficult to determine with precision, and at the highest strains single aggregates become indistinguishable as tectonic banding forms. The graph (Fig. 4a) shows a wide scatter of measurements at low strains, the spread of which decreases as the strain increases. Few points lie on the theoretical curve for simple shear (Ramsay 1967), although the correlation tends to improve as strain increases.

The shear strain parameter can be theoretically calculated for simple shear alone from the axial or strain ratio of the aggregates, using the following relationship (Ramsay 1967, Burg & Laurent 1978):

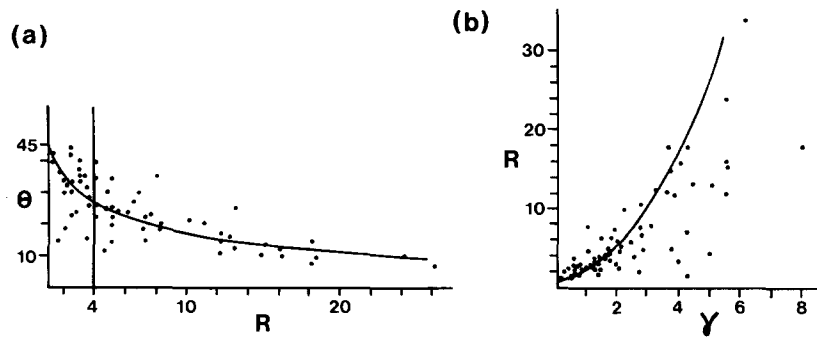


Fig. 4. (a) Finite strain ratios ( $R$ ) determined from polycrystalline mineral aggregates against long axis orientation ( $\theta$ ) of the aggregate relative to the shear zone boundary.  $\theta$  line for simple shear is shown (after Ramsay 1967); the vertical line at  $R = 4$  gives the maximum limit of ratios used by Coward (1976).

$$R = \frac{\gamma^2 + 2 + \gamma\sqrt{\gamma^2 + 4}}{2} \quad (2)$$

which approximates to

$$R = \gamma^2 + 2 \quad \text{when } \gamma > 3. \quad (3)$$

From these equations a simple shear curve can be drawn with which the measured  $\gamma$  and  $R$  readings for each aggregate can be compared (Fig. 4b). There is a wide scatter of points on the graph, with a large number plotting both below and well away from the simple shear curve.

As the studied specimen comes from a shear zone of finite length, it might be reasonable to expect a deviation from the ideal shear zone model involving simple shear over an infinite length (Coward 1976). Burg & Laurent (1978) however, satisfactorily accounted for the deformation within a small continuous shear zone, without necessary recourse to Coward's pure shear model.

As a preliminary working model, even after realizing measurement limitations, three factors suggest that the deformation of shear zone 1 involved a mechanism that approximated to simple shear.

(i) Along the length of the shear zone (42 cm) iso- $\gamma$  lines remain subparallel.

(ii) Across the  $Y$  axis similar contour patterns for  $\gamma$  values are reproducible (shown in Fig. 2) for  $\ln \gamma$  values.

(iii) Computed displacements (determined from the area under the strain-distance profiles, i.e. a simple shear approach, Fig. 3) at locations, both along the zone and at intervals across the  $Y$  axis suggest constant offset (values close to 16 cm).

Coward (1976, fig. 4) recognized major discrepancies between aggregate strain ratios and simple shear predicted  $\theta$  values. Figure 4(a) includes a line showing the maximum  $R$  readings used by Coward. At low strains scattered results identical to those of Coward are obtained. However, the improvement in correlation as strain increases ( $R$  becoming larger) means a closer agreement with simple shear deformation than that afforded by Coward's (p. 187) statement "the difference between measurements and the ratios predicted for simple shear alone are too great to be explained in this

way". Several explanations can account for this situation.

(1) The assumption of initial spherical and then ellipsoidal aggregate shapes necessarily involves errors; these errors are high at low strains but decrease with increasing strain.

(2) At the low strains the effect of the Coward pure shear components are still retained by the fabric but as the shear zone grows and deformation continues the superimposition of successive simple shear increments tends towards obscuring this effect.

(3) There is the possibility that some aggregates have suffered ductile boudinage or stress-transfer cracking because of ductility contrast between aggregate and matrix.

(4) Measurement errors; these are of two sorts. First, the technical difficulty of measuring large axial ratios with accuracy because of the loss of aggregate definition with the onset of banding. Secondly, aggregates with large strain ratios can depict the finite strain trajectory and be strongly curved and thinned towards the higher strain end.

(5) The few very low axial ratio aggregates may actually be 'semi-stable' up to medium strains.

## SHEAR ZONE MICROSTRUCTURE

### *Optical microstructure*

Part of shear zone 2 is shown in an  $XZ$  section (Fig. 5) which includes the deformed rock from the trace of the shear zone boundary plane to the shear zone centre. As elsewhere, this metagabbro comprises felsic and mafic polycrystalline aggregates. The main features associated with the deformation are listed, and the microstructural changes affecting the felsic aggregates with increasing strain are schematically shown in Fig. 6. Observations are made from shear zone 2 which is broadly similar to shear zone 1 in its microstructural development. The most distinctive microstructural feature is the grain size reduction accompanying the strain increase, shown by both plagioclase (Fig. 6) and hornblende (Fig. 5a). The felsic aggregates at the shear zone boundary (Figs. 5a &

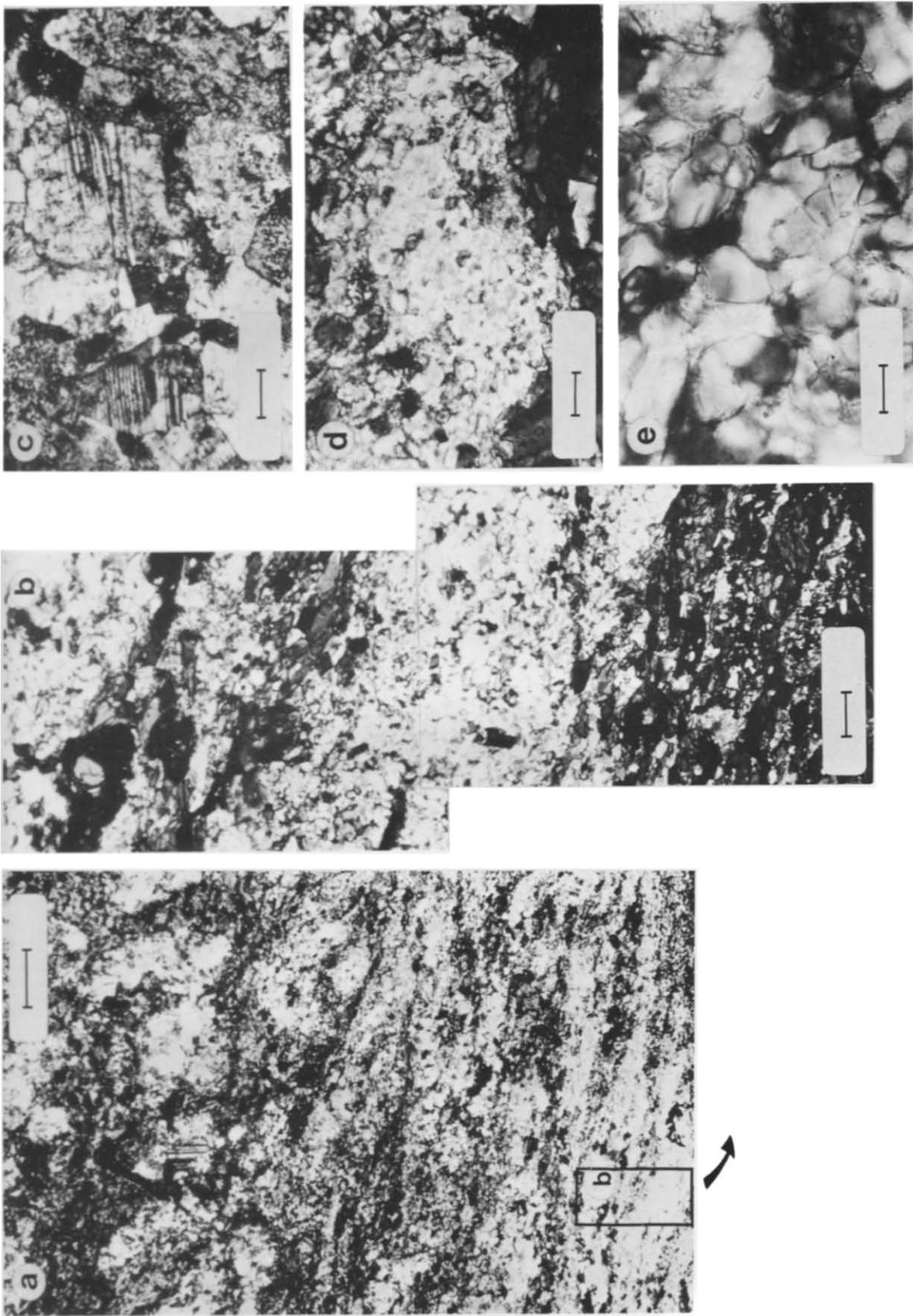


Fig. 5. Photomicrographs of shear zone 2; scale-bar lengths in microns except for Fig. 5a. (a) Part of the shear zone in XZ section showing grain size reduction and fabric development towards high strain region (bottom of photograph) (0.125 cm). (b) Enlargement of high-strain region of Fig. 5a; interlamination of essentially monomineralic layers of amphibole and feldspar (185). (c) Felsic aggregate at low strain showing coarse grain size, igneous twinning and no recrystallization in feldspar (170). (d) Subgrains and recrystallized grains in a polygonized feldspar at high strains;  $\gamma = 10$  (50). (e) Recrystallized feldspar at the shear zone centre; note small grain size and smooth boundaries, extinction usually sharp. 'Fuzziness' in photograph is natural and due to high magnification of a thick slide (25).



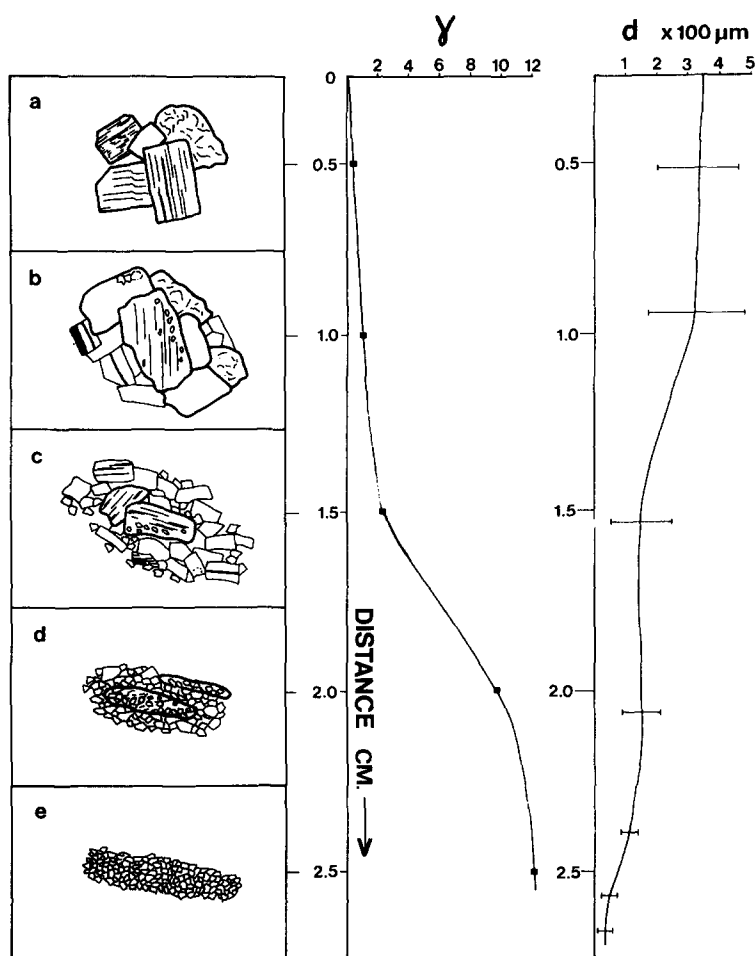


Fig. 6. Detail of feldspar microstructural development with increasing strain. (a) Aggregates at the shear zone boundary with coarse feldspars and igneous features plus minor kinking of polysynthetic twins. (b and c) Some feldspar subgrains and myrmekite. Smaller recrystallized and fresh feldspars common at grain margins. (d) Only relict primary feldspars remain, commonly polygonized in a groundmass of fresh feldspar. (e) Stable recrystallized feldspar microstructure is maintained. Microstructure relates directly to shear strain and grain size/distance graphs. Limit bars on the size/distance graph are for 1 standard deviation based on at least 50 measurements.

e) comprise coarse plagioclase crystals of varying size and orientation with some patchy sericite development and are typical of the metagabbro as a whole. At low strains there are few recrystallized feldspars (<10%) mainly at the margins of the primary igneous feldspars. As the finite strain increases, the percentage of recrystallized grains also increases until within the central regions the feldspar grains are 100% recrystallized.

The grain size/distance graphs (Fig. 6) give the mean size and size range of feldspars within the aggregates. At low strains the primary feldspars are coarse and variable in size. A continuous recrystallized grain size decrease accompanies strain increase until a 'stable' grain size of about  $18 \mu\text{m}$  width is achieved at  $\gamma$  values near 12. Concomitant with the grain size reduction is the lowering of the grain width standard deviation so that in the centre of the shear zone all the grains approach the stable size for the system.

Some relict igneous feldspars which persist, show undulatory extinction and can be distinguished in certain aggregates up to very high strains (e.g. Fig. 5d). Recrystallized feldspars can possess simple broad twins but they are more frequently untwinned. New feldspars are also remarkably free of alteration to sericite, particularly

at the smallest sizes, and no clinozoisite is developed. Streaks of assumed primary sericitized feldspar may form discontinuous envelopes around the amphibole layers at high strains.

Characteristic features of the stable feldspar within the highest strain areas, besides its small size, are its shape, grain boundary morphology and internal microstructure. These new grains (Fig. 5e) are rectangular or equidimensional in shape, possess smooth and gently curved boundary outlines and are comparatively (optically) strain free showing no, or at times only slight, undulatory extinction; though occasionally there is a hint of an additional much smaller subgrain structure. There is a slight but noticeable tendency for the primary igneous feldspars to contain exsolved droplets of clear quartz which increase in number with strain.

Amphiboles behave in a similar way to the feldspars but the mafic polycrystalline aggregates at low strains and even at the shear zone border are recrystallized to a small size (ca.  $100\text{--}200 \mu\text{m}$ ). That is, they are not the coarse primary metamorphic hornblendes. The hornblende shows a similar trend in grain size reduction, however the constant size recorded in the very high strain regions is slightly coarser than the feldspars, at

30  $\mu\text{m}$ . At this stage the amphibole prism faces are exceptionally well developed, forming almost equidimensional perfect diamond shapes, and distinct subgrain features are not obvious. Single or small clusters of hornblende are unevenly and sparsely interspersed with the stable feldspar grains at high strains.

There is a complete change in the fabric of the rock from outside to the centre of the shear zone. The border is marked by polycrystalline aggregates with a weak shape fabric; but parallel to the mylonitic foliation in the centre, essentially monomineralic layering has developed. These are subparallel mafic and felsic units giving a banded fabric to the rock (Figs. 5a & b).

### STRAIN RATE AND PALAEOSTRESS

In an ideal shear zone where ductile deformation is taken up across the full width of the zone, the shape of the strain profile after unit displacement must also resemble the strain rate profile, if all deformation is synchronous. If deformation is by diffusion creep the strain rate is inversely proportional to the grain size according to the following relationship given by White (1976).

$$\dot{\epsilon} = \frac{21DvV}{KTd^2} \left( \frac{1 + \pi SDb}{dDv} \right)^8. \quad (4)$$

Here  $\dot{\epsilon}$  = strain rate,  $Db$  = grain boundary diffusivity,  $V$  = activation volume,  $d$  = grain diameter,  $T$  = temperature in Kelvin,  $Dv$  = lattice diffusivity and  $K$  = Boltzman's constant. For lattice diffusion (Nabarro-Herring creep)  $\dot{\epsilon} \propto 1/d^2$  and for grain boundary diffusion (Coble creep)  $\dot{\epsilon} \propto 1/d^3$ . White (1979a, b, c) in a series of publications, details first the problems associated with palaeostress estimates and then the applicability of these estimates in demonstrating stress variations across ductile (mylonite) shear zones.

If deformation is by creep or hot working, the size of recrystallized grains and subgrains is stress dependent if grain boundary migration of 'foam' structure type can be specifically excluded (White 1979b). This relationship has considerable empirical support (Takeuchi & Argon 1976, Nicolas & Poirier 1976, Mercier *et al.* 1977, p. 213, White 1979c). It has been argued that recrystallized quartz grain sizes reflect the stresses operating at the time of recrystallization and the initiation of mylonite within shear zone centres then leads to a 'stress drop' or 'relaxation' (White 1977, 1979b, c, Schmid 1979).

The theoretically derived stress-grain size relationship of Twiss (1977, p. 236) is:

$$\sigma = Kdg^{-u} \quad (5)$$

where  $dg$  is the grain diameter and  $K$  and  $u$  are constants, whose respective values for anorthite are 7.8 and  $-0.68$ . Using this equation, stress values can be obtained increasing into shear zone 2 from 31 MPa (feldspar grain size = 130  $\mu\text{m}$ ) to 119 MPa (grain size 18  $\mu\text{m}$ ). These figures, of course, have only relative significance, not

only for the limitations expressed by White (1979a, b, c) for quartz, but also because the  $K$  value is valid only for anorthite and not andesine.

Where grain boundary sliding is suspected, whether it is within the superplastic domain or not, estimates for stress levels are likely to be in error as stress variations can then take place without a re-equilibration of grain size (White 1979a, Schmid 1979).

### VARIATIONS IN MINERAL CHEMISTRY

#### *Chemical changes with increasing strain*

This electron microprobe study was undertaken to detect any variations in mineral chemistry that would correlate with the deformation across the shear zones. Shear zone 2 provided an opportunity to make a continuous series of analyses at different distances and therefore varying finite strains, from the shear zone centre. From shear zone 1, a more direct comparison between low and high finite strains is possible, by selecting two thin sections (SZO and SZI) allowing, in each case, a number of analyses to be made at each finite strain state. The deformation within the shear zones took place under amphibolite facies conditions and over such small distances initial homogeneity of host rock composition can be assumed.

As elsewhere in the metagabbro, the recrystallization of feldspar is associated with a compositional change. Coarse labradorites ( $\text{An}_{57-59}$ ) recrystallize to calcic andesines ( $\text{An}_{45-49}$ ) and in shear zone 1, one result gave a sodic andesine ( $\text{An}_{34}$ ). This implies both release of silica and calcium though no epidote group minerals have grown.

Using the classification scheme of Leake (1978), the majority of the amphiboles are magnesio-hornblendes; three analyses from shear zone 2 plot just within the ferro-hornblende field and one pargasitic variety was recorded from shear zone 1. These hornblendes are optically unzoned and at first sight suggest isochemical behaviour throughout the deformation (e.g. Fig. 7) but in detail they reveal subtle variations.

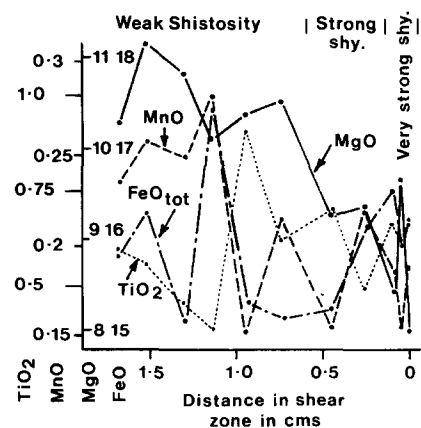


Fig. 7. Selected weight % element oxides from 11 amphibole analyses against distance in shear zone 2.



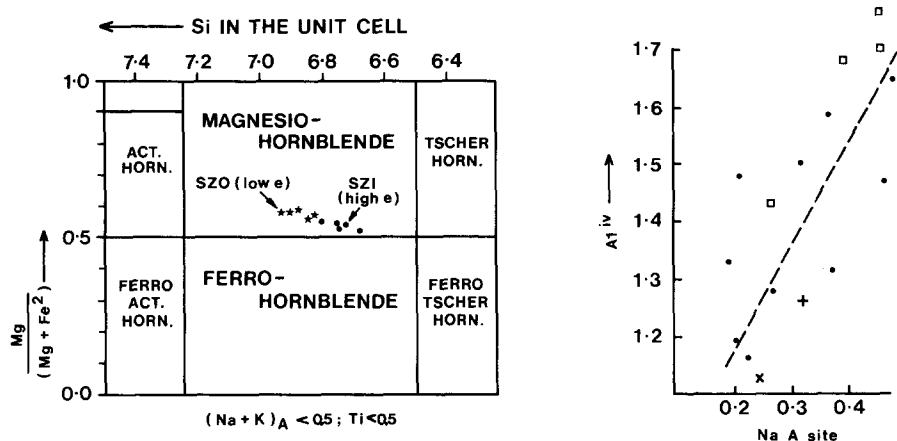


Fig. 8. (a) Amphiboles from shear zone 1 plotted on I.M.A. (1978) nomenclature diagram. (b) Plot of amphibole  $Al^{IV}$  content against  $Na_A$  site. Shear zone 1:  $\times$ , low strain (5 analyses); +, high strain (7 analyses); shear zone 2:  $\square$ , low strain;  $\bullet$ , high strain.

From Fig. 7 it can be seen that some irregular changes in composition occur across zone 2. Fluctuations are perhaps expected as amphiboles are notorious for showing variation about their mean compositions, Spray & Roddick (1980, p. 47). However, certain chemical trends correlate with the progressive deformation and are regarded as being of significance. These are the decrease in  $MgO$  and  $MnO$  and increase in  $A$  site occupancy into the shear zone (Fig. 8a).

Broadly the results of shear zone 1 (Table 1) concur in that there is a marked decrease in  $MgO$  and  $MnO$  and an increase in  $A$  site occupancy with strain. There are some differences however;  $CaO$  shows a slight decrease along with  $SiO_2$  and the total  $Fe$  oxide and  $Al_2O_3$  increase

significantly. The gain in aluminium is reflected both by the  $Al^{IV}$  and  $Al^{VI}$  contents (Table 1, Fig. 8a).

In both shear zones there is a trend towards decreasing the ratio of  $100 Mg/(Mg + Fe_{tot} + Mn)$  with strain. The mean values for shear zone 2 are 53.9, 50.9 and 48.8 in the low, medium and high strain areas, respectively and those from shear zone 1 range from 54.19 (low strain) to 49.8 (high strain).

Grapes *et al.* (1977) document many similar trends from within a gabbroic sequence in Japan. They describe the changes in amphibole chemistry during the alteration of a gabbroic amphibolite to schistose amphibolite with increased 'shearing' due to thrusting. Besides the  $Al^{IV}$ - $(NaK)_A$  relationship seen in the shear zones (Fig. 8b),

Table 1. Averaged amphibole compositions from shear zone 1

		SZ0 (low strain)		SZ1 (high strain)	
		Mean	S.D.	Mean	S.D.
	$SiO_2$	45.26	0.495	44.779	0.62
	$TiO_2$	0.688	0.087	0.676	0.156
	$Al_2O_3$	8.996	0.364	10.853	1.4
	$FeO_{tot.}$	16.498	0.151	17.676	0.8
	$MnO$	0.242	0.036	0.219	0.051
	$MgO$	11.14	0.187	9.992	0.548
	$CaO$	11.474	0.248	11.144	0.412
	$Na_2O$	0.876	0.2	1.078	0.326
	$K_2O$	0.202	0.21	0.242	0.019
Total		95.38		96.655	
T(Z) = 8	Si	6.878	0.0376	6.739	0.037
	$Al^{IV}$	1.122		1.261	
			0.063		0.21
C(Y) = 5	$Al^{VI}$	0.489		0.662	
	Ti	0.078	0.001	0.076	0.018
	Mn	0.031	0.004	0.028	0.007
	Mg	2.523	0.046	2.243	0.15
	$Fe^{2+}_{tot.}$	1.877		1.99	
			0.014		0.128
B(X) = 2	$Fe^{2+}_{tot.}$	0.22		0.23	
	CA	1.868	0.293	1.79	0.07
	Na	0.0		0.0	
			0.58		0.088
A = 0.1	Na	0.258		0.313	
	K	0.039	0.004	0.047	0.004

SZ0 (low strain) 5 analyses, SZ1 (high strain) 7 analyses. Structural formula calculations based on a total anion charge of  $-46$ , equivalent to 22 oxygens and 2 hydroxyl groups (Binns 1965).

there are other similarities with the Japanese amphiboles. The noted decrease in CaO with Fe enrichment and also the decrease in Mg and Si with Al and Fe enrichment are examples. This latter coupled trend favours the paired substitution  $Al^{IV}Fe^{3+} \rightleftharpoons MgSi$ , suggested by Kostyuk & Sobolev (1969) and is of particular relevance to shear zone 1. Grapes *et al.* (1977) graphically trace the decrease in the ratio  $100 Mg/(Mg + Fe_{tot} + Mn)$  with shearing which also correlates with an increase in A site occupancy and  $Al^{IV}$  with a decrease in Si.

The Mn and Mg decrease and the estimated behaviour of Fe in shear zone 2 supports the substitution relationship  $Fe^{2+} \rightleftharpoons Mn^{2+}, Mg^{2+}$  in the C or Y site. This cannot be an effect of host rock chemistry (Binns 1965, p. 318) but the substitution "may be strongly controlled by  $fO_2$ ", Spray & Williams (1980). The exact significance of changes in Mn distribution is apparently a little obscure but is probably greatly influenced by the Fe–Ti oxides (Grapes *et al.* 1977, p. 305).

## DISCUSSION

Both shear zones are characterized by strain profiles which show a broad region of low strain and a very narrow central region of high strain. Broadly, plane strain results from simple shear, and this is especially well shown at high strains. Strain softening processes operated in both shear zones, so localizing the deformation. Schmid (1979b), whilst accepting the importance of the strain softening phenomena, implied that there are two separate paths for shear zone development; (a) Softening occurs where deformation is greatest and "where a new and smaller grain size developed faster" or (b) Initial stress variations and concentrations lead to small equilibrium recrystallized grain sizes and subsequent softening. These are not thought of as necessarily competing or separate processes here.

### *Deformation mechanisms*

Investigations into the plastic properties of both amphibole and plagioclase are rather limited, though for the purposes of this paper features such as the postulated slip systems involved during dislocation creep of these minerals, need not be discussed (refer to Nicholas & Poirier 1976, pp. 191–200).

References to feldspar subgrains, particularly from granitoid rocks, are rare (e.g. Roshoff 1979, Allison *et al.* 1979). This may be due in part to crystal lattice constraints within sodic plagioclases, as subgrains are more common within andesines and labradorites from amphibolite facies terrains (White 1975, p. 299).

Subgrains from within andesines of these shear zones are rare at low strains; at high strains however, subgrains are abundant (12–20  $\mu m$ ) and completely polygonized grains occur (evidence of recovery). There is no single  $\gamma$  value at which the subgrains in each aggregate or within each feldspar, become common suggesting that their

appearance is not wholly controlled by finite strain state. The initial feldspar crystallographic orientation is likely to vary and some will be orientated for easier slip than others. This would be a form of geometric softening as explained by White *et al.* (1980) and Poirier (1980).

The often quoted grain size for quartz, below which rapid acceleration of strain rate occurs, is 10  $\mu m$  (e.g. White 1976, p. 82, 1977 p. 163 and fig. 5). In this respect, it must be noted that the size of steady state recrystallized grains for a given stress, of the minerals calcite, quartz, olivine and anorthite is predicted to be approximately the same, within a factor of two (Twiss 1977, p. 236). Using constants supplied by Twiss (1977) it can be seen that feldspar grains should equilibrate at a slightly smaller size than coexisting quartz and this agrees with the findings of White *et al.* (1980). The degree of strain softening also depends on the accommodating process for grain boundary sliding (White 1977, Etheridge & Wilkie 1979), but the microstructural evidence for particular accommodation processes can be somewhat ambiguous. As there is no direct supportive evidence in the literature to the contrary, it seems at first sight that the stable feldspar size of 18  $\mu m$  is not sufficiently small to produce the total strain softening of the zone by grain boundary sliding and Coble creep mechanisms. Three possibilities can be advanced for explanation of the strain softening.

(a) Grain boundary sliding can make a significant contribution to strain rate during the deformation of quartz, even when the grain size is sufficiently coarse for dislocation creep to be the dominant deforming mechanism (Regime III flow of Etheridge & Wilkie 1979). If this can also be applied in broad terms to feldspars, a similar situation may arise during their deformation.

(b) The value of the critical grain size may increase with grade of metamorphism (White 1977, p. 166) or perhaps these stringent sizes, often based on studies of metallurgical materials, may not be so 'critical' in geological environments.

(c) Continuous dynamic recrystallization can produce strain free nuclei.

Continuous recrystallization, where grains continually deform and then recrystallize, perhaps cyclically (White 1977, p. 164), results in a constant microstructure and grain size being maintained. This grain size can be much coarser than the stable grain size necessary for dominant grain boundary sliding and Coble creep. For example, Carreras *et al.* (1977) describe a quartz mylonite with stable microstructure at a grain size of 100  $\mu m$ . The formation of strain-free, new grains prevents strain hardening and leads to marked softening even if continued deformation of recrystallized grains is by dislocation processes (White 1977, White *et al.* 1980, Poirier 1980).

### *Ionic diffusion—the role of fluids*

The mineralogical changes, brought about during metamorphic dynamic recrystallization indicate local

conditions favourable for ionic diffusion or 'metamorphic differentiation' as termed by Grapes *et al.* (1977) and imply the activity of fluids. It has long been realized that shear zones may be paths for focused fluid flow during metamorphism (Beach & Fyfe 1972, p. 179). The grain size reduction accompanying dynamic recrystallization in a shear zone increases the surface area of the mineral grains and enhances the introduction of a fluid phase (Brodie 1980), by promoting the conditions necessary for diffusion and thereby drawing 'water' into the zone (Beach 1976, 1980).

As elsewhere (Beach 1976, 1980) a fluid phase may have been responsible for the removal of  $\text{Ca}^{2+}$ , which would have been released during the feldspar compositional changes, a factor together with the high temperature which can account for the absence of epidote group minerals. A supply of  $\text{K}^+$  is also needed to explain the increases in amphibole A site  $\text{K}^+$ .

The significance of the chemical changes, however minor, and the presence of a fluid phase, is that together, they make a further contribution to the process of strain softening. Although the study of the interrelationship between metamorphism and deformation has been rather neglected (White & Knipe 1978, p. 515), there is growing evidence for metamorphic processes during deformation forming an integral part of the strain softening. The influx of fluids initiates metamorphic reactions, resulting in small new grains that are strain free and consequently 'weaker' than the original grains thus bringing about "reaction-enhanced ductility", White & Knipe (1967), Beach (1980).

## REFERENCES

- Allison, I., Kerrich, R. & Starkey, J. 1979. Mineralogical changes in the transformation of granite to mylonite at Mieville, Switzerland. Abstract presented at Int. Conf. on Shear Zones in Rocks, Barcelona, Spain, 1979.
- Barrois, C. 1896. Legende de la feuille de Saint-Brieuc (No. 59 de la carte geologique de France au 1/80,000). *Annls Soc. géol. N.*, 66–87.
- Beach, A. 1976. The interrelations of fluid transport deformation, geochemistry and heat flow in early Proterozoic shear zones in the Lewisian Complex. *Phil. Trans. R. Soc.* **A280**, 569–604.
- Beach, A. 1980. Retrogressive metamorphic processes in shear zones with special reference to the Lewisian complex. *J. Struct. Geol.* **2**, 257–263.
- Beach, A. & Fyfe, W. S. 1972. Fluid transport and shear zones at Scourie, Sutherland: evidence of overthrusting? *Contr. Miner. Petrol.* **36**, 175–180.
- Binns, R. A. 1965. The mineralogy of metamorphosed basic rocks from the Willyama Complex, Broken Hill district, New South Wales. Parts 1 & 2. *Mineralog. Mag.* **35**, 306–326; part 2, **36**, 561–587.
- Brodie, K. H. 1980. Variations in mineral chemistry across a shear zone in phlogopite peridotite. *J. Struct. Geol.* **2**, 265–272.
- Burg, J. P. & Laurent, P. 1978. Strain analyses of a shear zone in a granulite. *Tectonophysics* **47**, 15–42.
- Carreras, J., Estrada, A. & White, S. 1977. The effects of folding on the *c*-axis fabrics of a quartz mylonite. *Tectonophysics* **39**, 3–24.
- Cogne, J. 1976. Carte Geologique Detaillee de la France, St. Brieuc, 3rd edn. 1:80,000.
- Coward, M. P. 1976. Strain within ductile shear zones. *Tectonophysics* **34**, 181–197.
- Etheridge, M. A. & Wilkie, J. C. 1979. Grain size reduction, grain boundary sliding and the flow strength of mylonites. *Tectonophysics* **58**, 159–178.
- Grapes, R. H., Hashimoto, S. & Miyashita, S. 1977. Amphiboles of a metagabbro-amphibolite sequence, Hidaka Metamorphic Belt, Hokkaido. *J. Petrology* **8**, 285–318.
- Hara, I., Takeda, K. & Kimura, T. 1973. Preferred lattice orientation of quartz in shear deformation. *Hiroshima Univ. J. Sci. Ser. C7*, 1–10.
- Kostyuk, E. A. & Sobolev, V. S. 1969. Paragenetic types of calciferous amphiboles of metamorphic rocks. *Lithos* **2**, 67–81.
- Leake, B. E. 1978. Subcommittee on the amphibole group: nomenclature of amphiboles. *Can. Mineralogist* **16**, 501–520.
- Leutwein, F., Sonet, J. & Zimmermann, J. L. 1968. Geochronologie et evolution orogenique Precambrienne et Hercynienne de la partie nord-est du Massif Armorica. *Mem. Sci. de la Terre* **11**, 1–84.
- Mercier, J. C. C., Anderson, D. A. & Carter, N. L. 1977. Stress in the lithosphere: inferences from steady state flow of rocks. *Pageophys.* **115**, 199–225.
- Miyashiro, A. 1978. *Metamorphism and Metamorphic Belts*. Allen & Unwin, London.
- Nicolas, A. & Poirier, J. P. 1976. *Crystalline Plasticity and Solid State Flow in Metamorphic Rocks*. Wiley, New York.
- Peach, B. N., Horne, J., Gunn, W., Clough, C. T., Hinxman, L. W. & Teall, J. J. H. 1907. The geological structure of the N.W. Highlands of Scotland. *Mem. geol. Surv. U.K.*
- Poirier, J. P. 1980. Shear localisation and shear instability in materials in the ductile field. *J. Struct. Geol.* **2**, 135–142.
- Ramsay, J. G. 1967. *Folding and Fracturing of Rocks*. McGraw-Hill, New York.
- Ramsay, J. G. & Graham, R. H. 1970. Strain variations in shear belts. *Can. J. Earth Sci.* **7**, 786–813.
- Roach, R. A. 1977. A review of the Precambrian rocks of the British Variscides and their relationship with the Precambrian of N.W. France. *Coll. Int. C.R.N.S., Rennes* **243**, 61–79.
- Roshoff, K. 1979. Microstructures in the Tannas augen gneiss, Scandinavian Caledonides. Abstract presented at Int. Conf. on Shear Zones in Rocks, Barcelona, Spain, 1979.
- Schmid, S. M. 1979. Shear zones in calcite rocks. Abstract presented at Int. Conf. on Shear Zones in Rocks, Barcelona, Spain, 1979.
- Spray, J. G. & Roddick, J. C. 1980. Petrology and  $^{40}\text{Ar}/^{39}\text{Ar}$  geochronology of some Hellenic sub-ophiolite metamorphic rocks. *Contr. Miner. Petrol.* **72**, 43–55.
- Spray, J. G. & Williams, G. D. 1980. The sub-ophiolite metamorphic rocks of the Ballantrae Igneous Complex, S.W. Scotland. *J. geol. Soc. Lond.* **137**, 359–368.
- Takeuchi, S. & Argon, A. S. 1976. Steady-state creep of single-phase crystalline matter at high temperature. *J. Mater. Sci.* **11**, 1542–1566.
- Teall, J. J. H. 1885. The metamorphosis of dolerite into hornblende schist. *Q. Jl geol. Soc. Lond.* **41**, 133–145.
- Thayer, T. P. 1980. Syncrystallization and subsolidus deformation in ophiolitic peridotite and gabbro. *Am. J. Sci.* **208**, 269–283.
- Twiss, R. J. 1977. Theory and applicability of a recrystallized grain size paleopiezometer. *Pageophys.* **115**, 227–244.
- White, S. 1976. The effects of strain on the microstructures, fabrics and deformation mechanism in quartzites. *Phil. Trans. R. Soc.* **A283**, 69–86.
- White, S. 1977. Geological significance of recovery and recrystallization processes in quartz. *Tectonophysics* **39**, 153–170.
- White, S. 1979a. Difficulties associated with palaeostress estimates. *Bull. Mineral.* **102**, 210–215.
- White, S. 1979b. Palaeo-stress estimates in the Moine Thrust Zone Eriboll, Scotland. *Nature, Lond.* **280**, 222–223.
- White, S. 1979c. Grain and sub-grain size variations across a mylonite zone. *Contr. Miner. Petrol.* **70**, 193–202.
- White, S. H. & Knipe, R. J. 1978. Transformation- and reaction-enhanced ductility in rocks. *J. geol. Soc. Lond.* **135**, 513–516.
- White, S. H., Burrows, S. E., Carreras, J., Shaw, N. D. & Humphreys, F. J. 1980. On mylonites in ductile shear zones. *J. Struct. Geol.* **2**, 175–188.